Vol 15 No 8, August 2006
1009-1963/2006/15(08)/1755-11

Chinese Physics

© 2006 Chin. Phys. Soc.
and IOP Publishing Ltd

Electromagnetic scattering from two parallel 2D targets arbitrarily located in a Gaussian beam*

Wang Yun-Hua(王运华)†, Guo Li-Xin(郭立新), and Wu Qiong(吴 琼)

School of Science, Xidian University, Xi'an 710071, *China*

(Received 11 January 2006; revised manuscript received 10 February 2006)

In this paper based on the equivalence principle and the reciprocity theorem, the scattered field up to second-order by two parallel 2D targets arbitrarily located in a Gaussian beam is considered. The first-order solution can easily be obtained by calculating the scattered field from isolated targets when illuminated by a Gaussian beam. However, because of the difficulty in formulating the couple scattering field, it is almost impossible to find an analytical solution for the second-order scattered field if the shapes of 2D targets are not canonical geometries. In order to overcome this problem, in this paper, the second-order solution is derived by using the technique based on the reciprocity theorem and the equivalence principle. Meanwhile, the relation between the secondary scattered field from target #1 and target #2 is obtained. Specifically, the bi- and mono-static scattering of Gaussian beam by two parallel adjacent inhomogeneous plasma-coated conducting circular cylinders is calculated and the dependence of attenuation of the scattering width on the thickness of the coated layer, electron number density, collision frequency and radar frequency is discussed in detail.

Keywords: reciprocity theorem, equivalence theorem, electromagnetic scattering, inhomogeneous plasma-coated conducting cylinders, Gaussian beam

PACC: 4120, 4110H

1. Introduction

It is well known that Gaussian beam can give a better simulation of radar beam than plane wave. Therefore, in recent years, the problem of scattering of a Gaussian beam by a composite scattering model has been the subject of extensive investigations. Because of the simplicity of the geometry and the interest in practical applications, scattering of plane wave or Gaussian beam by isolated cylinders or spheres has been well studied both theoretically and experimentally.[1−12] However, when the composite scattering field from discrete random media is studied, the interactions of electromagnetic wave between different scatterers should be taken into account. Because of the important influence on total field, higher-order scattered field has attracted the attention of many workers. Unfortunately, in order to obtain the scattering solution up to higher-order, it is necessary to treat the electromagnetic interactions between objects that are not only non-plane-wave in character but have non- uniformities in amplitude and phase. For this type of problem, the exact analytical solutions cannot be found except in a very small number of cases.[13−15] To overcome these difficulties, in this paper, an approximate solution for scattering field of a Gaussian beam from two parallel adjacent 2D targets is derived by employing the reciprocity theorem[16−19] and the equivalence principle.[19] And in the solution, only the first-order scattered field of one objects and the equivalent surface electric or/and magnetic current density induced by the incident beam on the other objects are required. Meanwhile, the relation between the secondary scattered field from target #1 and target #2 is discussed.

Because plasma can efficiently absorb electromagnetic waves, it can be used as microwave absorbers.[20−23] The absorption is dependent on several parameters such as the electron number density, the radar frequency, the thickness of the plasma layer, the momentum-transfer collision frequency, and so on. Therefore, in Section 4, the technique proposed in Section 2 is applied to obtain an approximate analytical solution for composite scattering field from two adjacent inhomogeneous plasma-coated conducting cylinders when they are illuminated by a Gaussian beam. In Section 5, the bi- and mono-static scattering is dis-

*Project supported by the National Natural Science Foundation of China (Grant No 60571058), the National Defense Foundation of China and Graduate Innovation Fund, Xidian University.

†E-mail: wyh78917@yahoo.com.cn

cussed and the results are compared with numerical computations based on the time domain integral equation method (TDIEM). The dependence of attenuation of the scattering width on the thickness of the coated layer, electron number density, collision frequency and radar frequency is discussed in detail.

2. Scattering of a Gaussian beam by two parallel adjacent 2D cylindrical objects

When we are interested in a limited region of space, it is well known that all uninteresting regions outside this space can be replaced by using equivalent sources, which include equivalent electric current and/or magnetic current.[19,24] In general, when the composite scattering field from two adjacent objects is studied, the field outside the objects is of interest. Thus, the dielectric objects can be replaced by using equivalent surface electric current and/or surface magnetic current. In this section, based on the equivalence principle and the reciprocity theorem, a solution for scattering of Gaussian beam by two adjacent 2D objects is derived. As shown in Fig.1(a), two adjacent parallel 2D objects are illuminated by Gaussian beam. Here, $\boldsymbol{E}_1^i$ and $\boldsymbol{H}_1^i$ denote the electric and magnetic field of the incident beam respectively. The incident Gaussian beam would induce an equivalent electric current density $\boldsymbol{J}_1$ and an equivalent magnetic current density $\boldsymbol{M}_1$ on the surface of 2D object #1 in the absence of 2D object #2. Firstly, considering the equivalent electric current density $\boldsymbol{J}_1$ as the primary source, we denote the electric and magnetic fields produced by $\boldsymbol{J}_1$ in the presence of object #2 by $\boldsymbol{E}_{J1}$ and $\boldsymbol{H}_{J1}$. On the other hand, considering the equivalent magnetic current density $\boldsymbol{M}_1$ as the excitation source, we denote the electric and magnetic fields produced by $\boldsymbol{M}_1$ in the presence of object #2 by $\boldsymbol{E}_{\mathrm{m}1}$ and $\boldsymbol{H}_{\mathrm{m}1}$.

Now, let us consider another situation where the source $\boldsymbol{J}_1$ and $\boldsymbol{M}_1$ are removed and a line electric current source $\boldsymbol{J}_{\mathrm{e}} = \hat{p}\delta(\boldsymbol{\rho} - \boldsymbol{\rho}_0)$ and a line magnetic current source $\boldsymbol{M}_{\mathrm{m}} = \hat{q}\delta(\boldsymbol{\rho} - \boldsymbol{\rho}_0)$ are placed at the far-zone observation point P as shown in Fig.1(b). Here, the unit polarization vector $\hat{q}(\hat{v}_{\mathrm{s}}$ or $\hat{h}_{\mathrm{s}})$ and $\hat{p}(\hat{v}_{\mathrm{s}}$ or $\hat{h}_{\mathrm{s}})$ are related by $\hat{q} = \hat{k}_{\mathrm{s}} \times \hat{p}$, where $\hat{k}_{\mathrm{s}}$ denotes the unit vector of the propagation direction of the scattering field. In the presence of object #2, the electromagnetic fields produced by $\boldsymbol{J}_{\mathrm{e}}$ and $\boldsymbol{M}_{\mathrm{m}}$ are denoted by $\boldsymbol{E}_{\mathrm{e}22}$, $\boldsymbol{H}_{\mathrm{e}22}$ and $\boldsymbol{E}_{\mathrm{m}22}$, $\boldsymbol{H}_{\mathrm{m}22}$ respectively. Here, we should note that the fields $\boldsymbol{E}_{\mathrm{e}22}$, $\boldsymbol{H}_{\mathrm{e}22}$, $\boldsymbol{E}_{\mathrm{m}22}$ and $\boldsymbol{H}_{\mathrm{m}22}$ not only contain the fields excited by the elementary line sources but also their scattering fields from object #2.

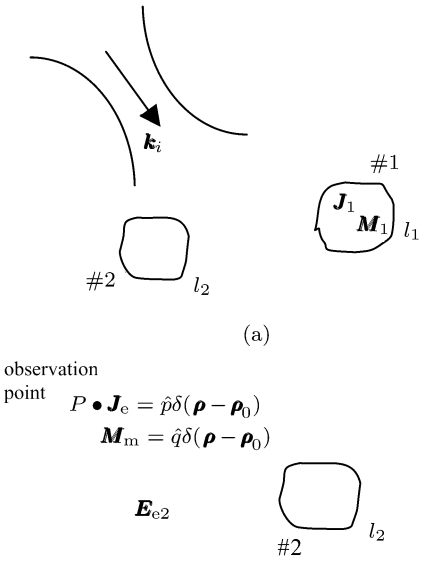


Fig.1. Cross-section of the scattering problem.

Application of the reaction theorem[19] over the entire 2D space results in

$$\begin{aligned}
&\int_{l_1} \boldsymbol{J}_1 \cdot (\boldsymbol{E}_{\mathrm{e}22} + \boldsymbol{E}_{\mathrm{m}22}) - \boldsymbol{J}_{\mathrm{e}} \cdot (\boldsymbol{E}_{J1} + \boldsymbol{E}_{\mathrm{m}1}) \\
&\quad + \boldsymbol{M}_{\mathrm{m}} \cdot (\boldsymbol{H}_{J1} + \boldsymbol{H}_{\mathrm{m}1}) - \boldsymbol{M}_1 \cdot (\boldsymbol{H}_{\mathrm{e}22} + \boldsymbol{H}_{\mathrm{m}22}) \mathrm{d}l \\
&= \oint\!\!\!\!\!\!\int_{l_\infty + l_2} [(\boldsymbol{E}_{J1} + \boldsymbol{E}_{\mathrm{m}1}) \times (\boldsymbol{H}_{\mathrm{e}22} + \boldsymbol{H}_{\mathrm{m}22}) \\
&\quad - (\boldsymbol{E}_{\mathrm{e}22} + \boldsymbol{E}_{\mathrm{m}22}) \times (\boldsymbol{H}_{J1} + \boldsymbol{H}_{\mathrm{m}1})] \cdot \mathrm{d}l\,. \qquad (1)
\end{aligned}$$

where l_∞ represents a closed circularity at infinity. At an infinite distance away from the source, the following two relations exist:

$$(\boldsymbol{E}_{J1} + \boldsymbol{E}_{\mathrm{m}1}) = -Z_0 \hat{n} \times (\boldsymbol{H}_{J1} + \boldsymbol{H}_{\mathrm{m}1})\,, \qquad (2)$$

$$(\boldsymbol{E}_{\mathrm{e}22} + \boldsymbol{E}_{\mathrm{m}22}) = -Z_0 \hat{n} \times (\boldsymbol{H}_{\mathrm{e}22} + \boldsymbol{H}_{\mathrm{m}22})\,. \qquad (3)$$

By substituting Eqs.(2) and (3) into Eq.(1), the integral over l_∞ on the right-hand side vanishes. Based on the equivalence principle and the extinction theorem,[19] the surface integral over the surface of object #2 also vanishes since $\hat{n} \times \boldsymbol{E} = \hat{n} \times \boldsymbol{H} = 0$. Thus, Eq.(1) can be written as

$$\int_{l_1} \boldsymbol{J}_1 \cdot (\boldsymbol{E}_{\mathrm{e}22} + \boldsymbol{E}_{\mathrm{m}22}) - \boldsymbol{J}_{\mathrm{e}} \cdot (\boldsymbol{E}_{J1} + \boldsymbol{E}_{\mathrm{m}1})$$

$$+ \boldsymbol{M}_{\mathrm{m}} \cdot (\boldsymbol{H}_{J1} + \boldsymbol{H}_{\mathrm{m1}}) - \boldsymbol{M}_1 \cdot (\boldsymbol{H}_{\mathrm{e22}} + \boldsymbol{H}_{\mathrm{m22}})\mathrm{d}l = 0. \quad (4)$$

Suppose that the two objects are both perfectly electric conducting scatterers, as well known, the surface magnetic current density is $\boldsymbol{M}_1 = 0$ and, based on the reciprocity theorem, the elementary magnetic current source $\boldsymbol{M}_{\mathrm{m}}$ is equal to zero, too. Then, Eq.(4) can be simplified as follows:

$$\int_{l_1} \boldsymbol{J}_1 \cdot \boldsymbol{E}_{\mathrm{e22}} - \boldsymbol{J}_{\mathrm{e}} \cdot \boldsymbol{E}_{J1}\mathrm{d}l = 0. \quad (5)$$

Suppose that two perfectly magnetic targets are considered, the surface electric current $\boldsymbol{J}_1 = 0$, and based on the reciprocity theorem, the elementary electric current source $\boldsymbol{J}_{\mathrm{e}}$ equal to zero, too. Then, Eq.(4) can be written as

$$\int_{l_1} \boldsymbol{M}_{\mathrm{m}} \cdot \boldsymbol{H}_{\mathrm{m1}} - \boldsymbol{M}_1 \cdot \boldsymbol{H}_{\mathrm{m22}}\mathrm{d}l = 0. \quad (6)$$

In the case that the two objects are both dielectric, using Eq.(4)–Eq.(6), we obtain the following three equations:

$$\int_{l_1} \boldsymbol{J}_1 \cdot \boldsymbol{E}_{\mathrm{e22}} - \boldsymbol{J}_{\mathrm{e}} \cdot \boldsymbol{E}_{J1}\mathrm{d}l = 0, \quad (7)$$

$$\int_{l_1} \boldsymbol{M}_{\mathrm{m}} \cdot \boldsymbol{H}_{\mathrm{m1}} - \boldsymbol{M}_1 \cdot \boldsymbol{H}_{\mathrm{m22}}\mathrm{d}l = 0, \quad (8)$$

$$\int_{l_1} \boldsymbol{J}_1 \cdot \boldsymbol{E}_{\mathrm{m22}} - \boldsymbol{J}_{\mathrm{e}} \cdot \boldsymbol{E}_{\mathrm{m1}} + \boldsymbol{M}_{\mathrm{m}} \cdot \boldsymbol{H}_{J1} - \boldsymbol{M}_1 \cdot \boldsymbol{H}_{\mathrm{e22}}\mathrm{d}l = 0. \quad (9)$$

Because $\boldsymbol{J}_{\mathrm{e}}$ and $\boldsymbol{M}_{\mathrm{m}}$ are both line sources, Eqs.(7) and (8) can also be written as the following forms:

$$\hat{p} \cdot \boldsymbol{E}_{J1} = \int_{l_1} \boldsymbol{J}_1 \cdot \boldsymbol{E}_{\mathrm{e22}}\mathrm{d}l, \quad (10)$$

$$\hat{q} \cdot \boldsymbol{H}_{\mathrm{m1}} = \int_{l_1} \boldsymbol{M}_1 \cdot \boldsymbol{H}_{\mathrm{m22}}\mathrm{d}l, \quad (11)$$

$$\hat{p} \cdot \boldsymbol{E}_{\mathrm{m1}} - \hat{q} \cdot \boldsymbol{H}_{J1} = \int_{l_1} \boldsymbol{J}_1 \cdot \boldsymbol{E}_{\mathrm{m22}} - \boldsymbol{M}_1 \cdot \boldsymbol{H}_{\mathrm{e22}}\mathrm{d}l. \quad (12)$$

Similarly, the sum of the first scattered field of object #2 and the second-order scattered field of object #1 can be evaluated by

$$\hat{p} \cdot \boldsymbol{E}_{J2} = \int_{l_2} \boldsymbol{J}_2 \cdot \boldsymbol{E}_{\mathrm{e11}}\mathrm{d}l, \quad (13)$$

$$\hat{q} \cdot \boldsymbol{H}_{\mathrm{m2}} = \int_{l_2} \boldsymbol{M}_2 \cdot \boldsymbol{H}_{\mathrm{m11}}\mathrm{d}l, \quad (14)$$

$$\hat{p} \cdot \boldsymbol{E}_{\mathrm{m2}} - \hat{q} \cdot \boldsymbol{H}_{J2} = \int_{l_2} \boldsymbol{J}_2 \cdot \boldsymbol{E}_{\mathrm{m11}} - \boldsymbol{M}_2 \cdot \boldsymbol{H}_{\mathrm{e11}}\mathrm{d}l. \quad (15)$$

In Eqs.(13)–(15), $\boldsymbol{E}_{\mathrm{e11}}$ denotes the field excited by the line electric current located at the observation point in the presence of object #1, and $\boldsymbol{H}_{\mathrm{m11}}$ corresponds to the line magnetic current. $\boldsymbol{J}_2$ and $\boldsymbol{M}_2$ are the equivalent electric and magnetic current density on the surface of object #2 induced by the incident Gaussian beam in the absence of object #1 respectively. Therefore, $\boldsymbol{E}_{J1} + \boldsymbol{E}_{\mathrm{m1}} + \boldsymbol{E}_{J2} + \boldsymbol{E}_{\mathrm{m2}}$ is the total scattered field of two dielectric objects up to second-order, and it can be evaluated by using Eqs.(10), (11), (13) and (14). Here, the relations $\boldsymbol{E}_{\mathrm{m1}} = -Z_0\hat{k}_{\mathrm{s}} \times \boldsymbol{H}_{\mathrm{m1}}$ and $\boldsymbol{E}_{\mathrm{m2}} = -Z_0\hat{k}_{\mathrm{s}} \times \boldsymbol{H}_{\mathrm{m2}}$ are used, where Z_0 is the characteristic impedance of free space.

3. The relation between the secondary scattered field from targets #1 and target #2

In section 2, using the reciprocity theorem and the equivalence principle, we obtain the secondary scattered fields from target #1 and #2. In this section, the relation between the secondary scattered fields is discussed.

The scattering interaction between two adjacent objects can be evaluated approximately by using the approach proposed in section 2. It is assumed that the equivalent electric and/or magnetic current on the surface of an isolated scatterer is the illumination source of the other scatterer and so on. Here it will be shown that the secondary scattered field emanated from target #2 can be obtained from the secondary scattered field emanated from target #1. Without loss of the generality, two adjacent dielectric targets in free-space illuminated by an incident wave are considered. Suppose that the induced equivalent electric and magnetic current density on the surface of target #1 in the he absence of object #2 are given by $\boldsymbol{J}_1$ and $\boldsymbol{M}_1$, then the scattered electric and magnetic field generated by $\boldsymbol{J}_1$ and $\boldsymbol{M}_1$ can be computed from the following two formulae:

$$\boldsymbol{E}_{1\mathrm{e}}^{\mathrm{s}} = \mathrm{i}k_0 Z_0 \int_{S_1} \bar{\bar{G}}(\boldsymbol{r}, \boldsymbol{r}')\boldsymbol{J}_1(\boldsymbol{r}')\mathrm{d}S' = \frac{-k_0 Z_0}{8\pi^2} \iint \frac{1}{k_z}(\bar{\bar{I}} - \hat{k}\hat{k}) \int_{S_1} \boldsymbol{J}_1(\boldsymbol{r}')\exp[\mathrm{j}\boldsymbol{k} \cdot (\boldsymbol{r} - \boldsymbol{r}')]\mathrm{d}S'\mathrm{d}k_x\mathrm{d}k_y\,, \quad (16)$$

$$\boldsymbol{H}_{1\mathrm{m}}^{\mathrm{s}} = \mathrm{i}k_0 Y_0 \int_{S_1} \bar{\bar{G}}(\boldsymbol{r},\boldsymbol{r}')\boldsymbol{M}_1(\boldsymbol{r}')\mathrm{d}S' = \frac{-k_0 Y_0}{8\pi^2}\iint \frac{1}{k_z}(\bar{\bar{I}}-\hat{k}\hat{k})\int_{S_1}\boldsymbol{M}_1(\boldsymbol{r}')\exp[\mathrm{j}\boldsymbol{k}\cdot(\boldsymbol{r}-\boldsymbol{r}')]\mathrm{d}S'\mathrm{d}k_x\mathrm{d}k_y\,, \quad (17)$$

where the second equality is resulted from the application of the 2D Fourier transform of the dyadic Green's function $\bar{\bar{G}}(\boldsymbol{r},\boldsymbol{r}')$. The subscript e and m represent the electric field deduced by $\boldsymbol{J}_1$ and the magnetic field deduced by $\boldsymbol{M}_1$ respectively. If the observation point is significantly apart from target #1, the recognized scattered electric field and field recognized can also be written as

$$\begin{aligned}\boldsymbol{E}_{\mathrm{e}}^{\mathrm{s}}(\hat{k}_i,\hat{k}) &= \mathrm{i}k_0 Z_0\int_{S_1}\bar{\bar{G}}(\boldsymbol{r},\boldsymbol{r}')\boldsymbol{J}_1(\boldsymbol{r}')\mathrm{d}S' \\ &= \frac{\mathrm{i}k_0 Z_0\mathrm{e}^{\mathrm{i}k_0 r}}{4\pi r}(\bar{\bar{I}}-\hat{k}\hat{k})\int_{S_1}\boldsymbol{J}_1(\boldsymbol{r}')\exp(-\mathrm{j}\boldsymbol{k}\cdot\boldsymbol{r}')\mathrm{d}S' = \frac{\mathrm{e}^{\mathrm{i}k_0 r}}{r}\mathrm{e}^{\mathrm{i}k_0(\hat{k}_i-\hat{k})\cdot\boldsymbol{r}_1}\bar{\bar{S}}_{1\mathrm{e}}(\hat{k}_i,\hat{k})\boldsymbol{E}_i\,, \quad (18)\\ \boldsymbol{H}_{\mathrm{m}}^{\mathrm{s}}(\hat{k}_i,\hat{k}) &= \mathrm{i}k_0 Y_0\int_{S_1}\bar{\bar{G}}(\boldsymbol{r},\boldsymbol{r}')\boldsymbol{M}_1(\boldsymbol{r}')\mathrm{d}S' \\ &= \frac{\mathrm{i}k_0 Y_0\mathrm{e}^{\mathrm{i}k_0 r}}{4\pi r}(\bar{\bar{I}}-\hat{k}\hat{k})\int_{S_1}\boldsymbol{M}_1(\boldsymbol{r}')\exp(-\mathrm{j}\boldsymbol{k}\cdot\boldsymbol{r}')\mathrm{d}S' = \frac{\mathrm{e}^{\mathrm{i}k_0 r}}{r}\mathrm{e}^{\mathrm{i}k_0(\hat{k}_i-\hat{k})\cdot\boldsymbol{r}_1}\bar{\bar{S}}_{1\mathrm{m}}(\hat{k}_i,\hat{k})\boldsymbol{H}_i\,, \quad (19)\end{aligned}$$

where $\hat{k}_i$ and $\hat{k}$ are the incident and scattering directions respectively. $\bar{\bar{S}}_{1\mathrm{e}}(\hat{k}_i,\hat{k})$ and $\bar{\bar{S}}_{1\mathrm{m}}(\hat{k}_i,\hat{k})$ are the bistatic scattering electric field amplitude matrix vector and magnetic amplitude matrix vector of target #1 and $\boldsymbol{r}_1$ is the position vector of target #1. Using Eqs.(18) and (19), we can obtain

$$\frac{\mathrm{i}k_0 Z_0}{4\pi}(\bar{\bar{I}}-\hat{k}\hat{k})\int_{S_1}\boldsymbol{J}_1(\boldsymbol{r}')\exp(-\mathrm{j}\boldsymbol{k}\cdot\boldsymbol{r}')\mathrm{d}S' = \mathrm{e}^{\mathrm{i}k_0(\hat{k}_i-\hat{k})\cdot\boldsymbol{r}_1}\bar{\bar{S}}_{1\mathrm{e}}(\hat{k}_i,\hat{k})\boldsymbol{E}_i, \quad (20)$$

$$\frac{\mathrm{i}k_0 Y_0}{4\pi}(\bar{\bar{I}}-\hat{k}\hat{k})\int_{S_1}\boldsymbol{M}_1(\boldsymbol{r}')\exp(-\mathrm{j}\boldsymbol{k}\cdot\boldsymbol{r}')\mathrm{d}S' = \mathrm{e}^{\mathrm{i}k_0(\hat{k}_i-\hat{k})\cdot\boldsymbol{r}_1}\bar{\bar{S}}_{1\mathrm{m}}(\hat{k}_i,\hat{k})\boldsymbol{H}_i. \quad (21)$$

Then, substituting Eq.(20) into Eq.(16) and Eq.(21) into Eq.(17), we can write the field $\boldsymbol{E}_{1\mathrm{e}}^{\mathrm{s}}$ and $\boldsymbol{H}_{1\mathrm{m}}^{\mathrm{s}}$

$$\begin{aligned}\boldsymbol{E}_{1\mathrm{e}}^{\mathrm{s}} &= \mathrm{i}k_0 Z_0\int_{S_1}\bar{\bar{G}}(\boldsymbol{r},\boldsymbol{r}')\boldsymbol{J}_1(\boldsymbol{r}')\mathrm{d}S' = \frac{\mathrm{i}}{2\pi}\iint\frac{1}{k_z}\exp(\mathrm{j}\,\boldsymbol{k}\cdot\boldsymbol{r})\frac{\mathrm{i}k_0 Z_0}{4\pi}(\bar{\bar{I}}-\hat{k}\hat{k})\int_{S_1}\boldsymbol{J}_1(\boldsymbol{r}')\exp(-\mathrm{j}\,\boldsymbol{k}\,\boldsymbol{r}')\mathrm{d}S'\mathrm{d}k_x\mathrm{d}k_y \\ &= \frac{\mathrm{i}}{2\pi}\iint\frac{1}{k_z}\exp(\mathrm{j}\boldsymbol{k}\cdot\boldsymbol{r})\mathrm{e}^{\mathrm{i}k_0(\hat{k}_i-\hat{k})\cdot\boldsymbol{r}_1}\bar{\bar{S}}_{1\mathrm{e}}(\hat{k}_i,\hat{k})\mathrm{d}k_x\mathrm{d}k_y\cdot\boldsymbol{E}_i\,, \quad (22)\\ \boldsymbol{H}_{1\mathrm{m}}^{\mathrm{s}} &= \mathrm{i}k_0 Y_0\int_{S_1}\bar{\bar{G}}(\boldsymbol{r},\boldsymbol{r}')\boldsymbol{M}_1(\boldsymbol{r}')\mathrm{d}S' = \frac{\mathrm{i}}{2\pi}\iint\frac{1}{k_z}\exp(\mathrm{j}\boldsymbol{k}\cdot\boldsymbol{r})\frac{\mathrm{i}k_0 Y_0}{4\pi}(\bar{\bar{I}}-\hat{k}\hat{k})\int_{S_1}\boldsymbol{M}_1(\boldsymbol{r}')\exp(-\mathrm{j}\boldsymbol{k}\,\boldsymbol{r}')\mathrm{d}S'\mathrm{d}k_x\mathrm{d}k_y \\ &= \frac{\mathrm{i}}{2\pi}\iint\frac{1}{k_z}\exp(\mathrm{j}\boldsymbol{k}\cdot\boldsymbol{r})\mathrm{e}^{\mathrm{i}k_0(\hat{k}_i-\hat{k})\cdot\boldsymbol{r}_1}\bar{\bar{S}}_{1\mathrm{m}}(\hat{k}_i,\hat{k})\mathrm{d}k_x\mathrm{d}k_y\cdot\boldsymbol{H}_i. \quad (23)\end{aligned}$$

In Eqs.(22) and (23), the near field scattered from target #1 is expanded in terms of a spectrum of plane waves. Then, using $\boldsymbol{E}_{1\mathrm{e}}^{\mathrm{s}}$ and $\boldsymbol{H}_{1\mathrm{m}}^{\mathrm{s}}$ as the illuminating fields, we can compute the secondary scattered field from target #2 in the far-field region from the following formulae:

$$\boldsymbol{E}_{21\mathrm{e}}^{\mathrm{s}} = \frac{\mathrm{e}^{\mathrm{i}k_0 r}}{r}\Big\{\frac{\mathrm{i}}{2\pi}\iint\frac{1}{k_z}\mathrm{e}^{\mathrm{i}k_0(\hat{k}_i-\hat{k})\cdot\boldsymbol{r}_1}\mathrm{e}^{\mathrm{i}k_0(\hat{k}-\hat{k}_{\mathrm{s}})\cdot\boldsymbol{r}_2}\bar{\bar{S}}_{1\mathrm{e}}(\hat{k}_i,\hat{k})\bar{\bar{S}}_{2e}(\hat{k},\hat{k}_{\mathrm{s}})\mathrm{d}k_x\mathrm{d}k_y\Big\}\cdot\boldsymbol{E}_i = \frac{\mathrm{e}^{\mathrm{i}k_0 r}}{r}\bar{\bar{S}}_{21\mathrm{e}}(\hat{k}_i,\hat{k}_{\mathrm{s}})\cdot\boldsymbol{E}_i, \quad (24)$$

$$\boldsymbol{H}_{21\mathrm{m}}^{\mathrm{s}} = \frac{\mathrm{e}^{\mathrm{i}k_0 r}}{r}\Big\{\frac{\mathrm{i}}{2\pi}\iint\frac{1}{k_z}\mathrm{e}^{\mathrm{i}k_0(\hat{k}_i-\hat{k})\cdot\boldsymbol{r}_1}\mathrm{e}^{\mathrm{i}k_0(\hat{k}-\hat{k}_{\mathrm{s}})\cdot\boldsymbol{r}_2}\bar{\bar{S}}_{1\mathrm{m}}(\hat{k}_i,\hat{k})\bar{\bar{S}}_{2\mathrm{m}}(\hat{k},\hat{k}_{\mathrm{s}})\mathrm{d}k_x\mathrm{d}k_y\Big\}\cdot\boldsymbol{H}_i = \frac{\mathrm{e}^{\mathrm{i}k_0 r}}{r}\bar{\bar{S}}_{21\mathrm{m}}(\hat{k}_i,\hat{k}_{\mathrm{s}})\cdot\boldsymbol{H}_i, \quad (25)$$

where $\bar{\bar{S}}_{2\mathrm{e}}(\hat{k},\hat{k}_{\mathrm{s}})$ and $\bar{\bar{S}}_{2\mathrm{m}}(\hat{k},\hat{k}_{\mathrm{s}})$ denotes the bistatic scattering matrix of target #2 and $\boldsymbol{r}_2$ is the vector position of target #2. Employing the similar method, we can obtain the secondary scattered field from target #1 as

$$\begin{aligned}\boldsymbol{E}_{12\mathrm{e}}^{\mathrm{s}} &= \frac{\mathrm{e}^{\mathrm{i}k_0 r}}{r}\Big\{\frac{\mathrm{i}}{2\pi}\iint\frac{1}{k_z}\mathrm{e}^{\mathrm{i}k_0(-\hat{k}-\hat{k}_{\mathrm{s}})\cdot\boldsymbol{r}_1}\mathrm{e}^{\mathrm{i}k_0(\hat{k}+\hat{k}_i)\cdot\boldsymbol{r}_2}\bar{\bar{S}}_{1\mathrm{e}}(-\hat{k},\hat{k}_{\mathrm{s}})\bar{\bar{S}}_{2\mathrm{e}}(\hat{k}_i,-\hat{k})\mathrm{d}k_x\mathrm{d}k_y\Big\}\cdot\boldsymbol{E}_i \\ &= \frac{\mathrm{e}^{\mathrm{i}k_0 r}}{r}\bar{\bar{S}}_{12\mathrm{e}}(\hat{k}_i,\hat{k}_{\mathrm{s}})\cdot\boldsymbol{E}_i, \quad (26)\\ \boldsymbol{H}_{12\mathrm{m}}^{\mathrm{s}} &= \frac{\mathrm{e}^{\mathrm{i}k_0 r}}{r}\Big\{\frac{\mathrm{i}}{2\pi}\iint\frac{1}{k_z}\mathrm{e}^{\mathrm{i}k_0(-\hat{k}-\hat{k}_{\mathrm{s}})\cdot\boldsymbol{r}_1}\mathrm{e}^{\mathrm{i}k_0(\hat{k}+\hat{k}_i)\cdot\boldsymbol{r}_2}\bar{\bar{S}}_{1\mathrm{m}}(-\hat{k},\hat{k}_{\mathrm{s}})\bar{\bar{S}}_{2\mathrm{m}}(\hat{k}_i,-\hat{k})\mathrm{d}k_x\mathrm{d}k_y\Big\}\cdot\boldsymbol{H}_i\end{aligned}$$

$$= \frac{\mathrm{e}^{\mathrm{i}k_0 r}}{r}\bar{\bar{S}}_{12\mathrm{m}}(\hat{k}_i, \hat{k}_\mathrm{s}) \cdot \boldsymbol{H}_i. \tag{27}$$

Comparing Eq.(24) with Eq.(26) and Eq.(25) with Eq.(27), we can easily show that

$$\bar{\bar{S}}_{21\mathrm{e}}(\hat{k}_i, \hat{k}_\mathrm{s}) = \bar{\bar{S}}^{(-\mathrm{t})}_{12\mathrm{e}}(-\hat{k}_\mathrm{s}, -\hat{k}_i) \quad , \qquad \bar{\bar{S}}_{21\mathrm{m}}(\hat{k}_i, \hat{k}_\mathrm{s}) = \bar{\bar{S}}^{(-\mathrm{t})}_{12\mathrm{m}}(-\hat{k}_\mathrm{s}, -\hat{k}_i), \tag{28}$$

where Eq.(28) results from the application of the following equalities:

$$\bar{\bar{S}}_{1\mathrm{e}}(\hat{k}, \hat{k}_\mathrm{s}) = \bar{\bar{S}}^{(-\mathrm{t})}_{1\mathrm{e}}(-\hat{k}_\mathrm{s}, -\hat{k}), \qquad \bar{\bar{S}}_{2\mathrm{e}}(\hat{k}_i, \hat{k}) = \bar{\bar{S}}^{(-\mathrm{t})}_{1\mathrm{e}}(-\hat{k}, -\hat{k}_i), \tag{29}$$

$$\bar{\bar{S}}_{1\mathrm{m}}(\hat{k}, \hat{k}_\mathrm{s}) = \bar{\bar{S}}^{(-\mathrm{t})}_{1\mathrm{m}}(-\hat{k}_\mathrm{s}, -\hat{k}), \qquad \bar{\bar{S}}2\mathrm{m}(\hat{k}_i, \hat{k}) = \bar{\bar{S}}^{(-\mathrm{t})}_{1\mathrm{m}}(-\hat{k}, -\hat{k}_i), \tag{30}$$

and the superscript (- t) denotes the matrix transposing and multiplying the off-diagonal elements by -1.

It is well known that the secondary electric field from target #2 and #1 can be written as

$$\boldsymbol{E}^\mathrm{s}_{12} = \boldsymbol{E}^\mathrm{s}_{12\mathrm{e}} - Z_0\hat{k}_\mathrm{s} \times \boldsymbol{H}^\mathrm{s}_{12\mathrm{m}}, \tag{31}$$

$$\boldsymbol{E}^\mathrm{s}_{21} = \boldsymbol{E}^\mathrm{s}_{21\mathrm{e}} - Z_0\hat{k}_\mathrm{s} \times \boldsymbol{H}^\mathrm{s}_{21\mathrm{m}}. \tag{32}$$

Therefore, using Eqs.(28)–(32), one can easily obtain the following relation:

$$\bar{\bar{S}}_{21}(\hat{k}_i, \hat{k}_\mathrm{s}) = \bar{\bar{S}}^{(-\mathrm{t})}_{12}(-\hat{k}_\mathrm{s}, -\hat{k}_i). \tag{33}$$

In the backscattering direction, $\hat{k}_i = -\hat{k}_\mathrm{s}$, then using Eq.(33), we can obtain that

$$\bar{\bar{S}}_{21}(\hat{k}_i, -\hat{k}_i) = \bar{\bar{S}}^{(-\mathrm{t})}_{12}(\hat{k}_i, -\hat{k}_i). \tag{34}$$

Equations(33) and (34) show that the secondary scattered field emanated from target #2 can be obtained from the secondary scattered field emanated from target #1.

4. Electromagnetic scattering of Gaussian beam by two parallel adjacent plasma-coated conducting cylinders

In the previous section, we have derived the expressions which can be applied to evaluate the scattered field from two any adjacent 2D objects with known geometries and dielectric properties. In this calculation we only require the scattered fields and equivalent surface currents of individual objects when illuminated by a Gaussian beam. As an example of the application of the new technology, in this section an approximate analytical solution is derived for two plasma-coated cylinders whose axes are parallel to x-axis. Firstly, an assumption is made that the two multilayered cylinders lie in the far-field region of each other, i.e., the following conditions should be satisfied:

$$\frac{2r_1^2}{\lambda} < \tilde{\rho}, \qquad \frac{2r_2^2}{\lambda} < \tilde{\rho}, \tag{35}$$

where λ denotes the wavelength of the incident wave, r_1 and r_2 are the radii of cylinder #1 and #2 respectively. Suppose a Gaussian beam, which propagates along the positive z-direction, is incident on the cylinder-cylinder pair. As shown in Fig.2, the incident Gaussian beam has its focal point at origin point and W_0 denotes its beam-waist radius.

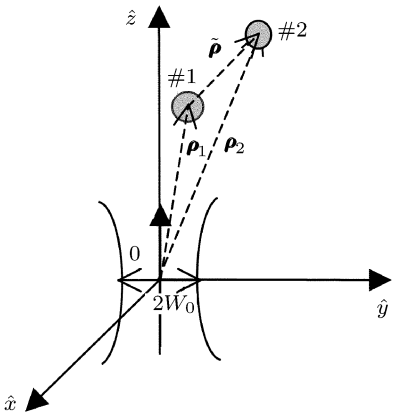


Fig.2. Geometry and coordinate of the scattering model.

Neglect the time factor $\exp(-\mathrm{i}\omega t)$, the spatial distribution of the amplitude of the electric component $E_{\hat{\eta}}$ in the $z = 0$ plane is given by[1]

$$E_{\hat{\eta}}(x, y, 0) = E_0 \exp[-y^2/W_0^2], \tag{36}$$

where E_0 denotes the amplitude of the electric component at the centre of the beam and, in the following, E_0 is assumed to be 1. W_0 is the beam-waist radius.

The polarization vector $\hat{\eta}$ may be chosen to be either $\hat{x}$ (TM) or $\hat{y}$ (TE).

Now, we derive the approximate analytical solutions of scattered field of the Gaussian beam by the cylinder–cylinder pair.

Since $\boldsymbol{E}_{\mathrm{e22}}$ and $\boldsymbol{H}_{\mathrm{m22}}$ are both composed of two components, Eqs.(10) and (11) can be divided into two parts, i.e.

$$\begin{aligned}\hat{p}\cdot\boldsymbol{E}_{J1} &= \int_{l_1}\boldsymbol{J}_1\cdot\boldsymbol{E}_{\mathrm{e22}}\mathrm{d}l = \int_{l_1}\boldsymbol{J}_1\cdot(\boldsymbol{E}_{\mathrm{ed}}+\boldsymbol{E}_{\mathrm{e2s}})\mathrm{d}l\\ &= \int_{l_1}\boldsymbol{J}_1\cdot\boldsymbol{E}_{\mathrm{ed}}\mathrm{d}l + \int_{l_1}\boldsymbol{J}_1\cdot\boldsymbol{E}_{\mathrm{e2c}}\mathrm{d}l\\ &= \hat{p}\cdot\boldsymbol{E}^{\mathrm{s}}_{J1\mathrm{d}} + \hat{p}\cdot\boldsymbol{E}^{\mathrm{s}}_{J12\mathrm{c}}\,, \qquad (37)\\ \hat{q}\cdot\boldsymbol{H}_{\mathrm{m1}} &= \int_{l_1}\boldsymbol{M}_1\cdot\boldsymbol{H}_{\mathrm{m22}}\mathrm{d}l\\ &= \int_{l_1}\boldsymbol{M}_1\cdot(\boldsymbol{H}_{\mathrm{md}}+\boldsymbol{H}_{\mathrm{m2s}})\mathrm{d}l\\ &= \int_{l_1}\boldsymbol{M}_1\cdot\boldsymbol{H}_{\mathrm{md}}\mathrm{d}l + \int_{l_1}\boldsymbol{M}_1\cdot\boldsymbol{H}_{\mathrm{m2c}}\mathrm{d}l\\ &= \hat{q}\cdot\boldsymbol{H}^{\mathrm{s}}_{\mathrm{m1d}} + \hat{q}\cdot\boldsymbol{H}^{\mathrm{s}}_{\mathrm{m12c}}\,, \qquad (38)\end{aligned}$$

where $\boldsymbol{E}_{\mathrm{ed}}$ is the direct electric field generated by $\boldsymbol{J}_{\mathrm{e}} = \hat{p}\delta(\boldsymbol{\rho}-\boldsymbol{\rho}_0)$ and $\boldsymbol{H}_{\mathrm{md}}$ is the direct magnetic field excited by $\boldsymbol{M}_{\mathrm{m}} = \hat{q}\delta(\boldsymbol{\rho}-\boldsymbol{\rho}_0)$. $\boldsymbol{E}_{\mathrm{e2c}}$ and $\boldsymbol{H}_{\mathrm{m2c}}$ are the scattered fields from cylinder #2 when illuminated by $\boldsymbol{E}_{\mathrm{ed}}$ and $\boldsymbol{H}_{\mathrm{md}}$ respectively. When the observation point $\boldsymbol{\rho}_0$ is in the far-field zone, the expressions of $\boldsymbol{E}_{\mathrm{ed}}$ and $\boldsymbol{H}_{\mathrm{md}}$ along $-\hat{k}_{\mathrm{s}}$ are given by[25]

$$\begin{aligned}\boldsymbol{E}_{\mathrm{ed}}(\rho_0) &= \frac{-k_0Z_0}{4}H_0^{(1)}(k_0\rho_0)\\ &\quad\times\exp(-\mathrm{i}\boldsymbol{k}_{\mathrm{s}}\cdot\boldsymbol{\rho})\hat{k}_{\mathrm{s}}\times\hat{k}_{\mathrm{s}}\times\hat{p}, \qquad (39)\\ \boldsymbol{H}_{\mathrm{md}}(\rho_0) &= \frac{-k_0Y_0}{4}H_0^{(1)}(k_0\rho_0)\\ &\quad\times\exp(-\mathrm{i}\boldsymbol{k}_{\mathrm{s}}\cdot\boldsymbol{\rho})\hat{k}_{\mathrm{s}}\times\hat{k}_{\mathrm{s}}\times\hat{q}, \qquad (40)\end{aligned}$$

where $\hat{k}_{\mathrm{s}}$ denotes the propagation direction of the scattered field, k_0 is the wave number of the incident wave in free space.

By invoking the equivalent principle, suppose that the equivalent electric and magnetic current density on the surface of cylinder #1 are denoted by $\boldsymbol{J}_1$ and $\boldsymbol{M}_1$ respectively, using Eqs.(37) and (38), we obtain the following two equations:

$$\hat{p}\cdot\boldsymbol{E}^{\mathrm{s}}_{J1\mathrm{d}} = \int_{l_1}\boldsymbol{J}_1\cdot\boldsymbol{E}_{\mathrm{ed}}\mathrm{d}l\,, \qquad (41)$$

$$\hat{q}\cdot\boldsymbol{H}^{\mathrm{s}}_{\mathrm{m1d}} = \int_{l_1}\boldsymbol{M}_1\cdot\boldsymbol{H}_{\mathrm{md}}\mathrm{d}l. \qquad (42)$$

Substituting Eqs.(39) and (40) into Eqs.(41) and (42), and using the Stratton–Thu formulation,[19] we get the first-order scattering field from cylinder #1 when illuminated by the incident Gaussian beam:

$$\begin{aligned}\hat{p}\cdot\boldsymbol{E}^{\mathrm{s}}_{1\mathrm{c}}(\boldsymbol{r}) &= \hat{p}\cdot(\boldsymbol{E}^{\mathrm{s}}_{J1\mathrm{d}}+\boldsymbol{E}^{\mathrm{s}}_{\mathrm{m1d}}) = \frac{-k_0Z_0}{4}H_0^{(1)}(k_0\rho_0)\cdot\exp(-\mathrm{i}\boldsymbol{k}_{\mathrm{s}}\cdot\boldsymbol{\rho}_1)\\ &\quad\hat{p}\cdot\Big[-\hat{k}_{\mathrm{s}}\times\hat{k}_{\mathrm{s}}\times\int_{l_1}\boldsymbol{J}_1\exp(-\mathrm{i}\boldsymbol{k}_{\mathrm{s}}\cdot\boldsymbol{\rho}')\mathrm{d}l' - Z_0\hat{k}_{\mathrm{s}}\times\int_{l_1}\boldsymbol{M}_1\exp(-\mathrm{i}\boldsymbol{k}_{\mathrm{s}}\cdot\boldsymbol{\rho}')\mathrm{d}l'\Big]\\ &= H_0^{(1)}(k_0\rho_0)\exp(-\mathrm{i}\boldsymbol{k}_{\mathrm{s}}\cdot\boldsymbol{\rho}_1+\mathrm{i}\boldsymbol{k}_i\cdot\boldsymbol{\rho}_1)\hat{p}\cdot\bar{S}_1^{\mathrm{g}}(\hat{k}_i,\hat{k}_{\mathrm{s}}). \qquad (43)\end{aligned}$$

In Eq.(43) the relation $\boldsymbol{E}^{\mathrm{s}}_{\mathrm{m1d}} = -Z_0\hat{k}_{\mathrm{s}}\times\boldsymbol{H}^{\mathrm{s}}_{\mathrm{m1d}}$ is used. $\bar{S}_1^{\mathrm{g}}(\hat{k}_i,\hat{k}_{\mathrm{s}})$, the bi-static scattered electric field amplitude vector of cylinder #1 when it is illuminated by the Gaussian beam, can be expressed as

$$\bar{S}_1^{\mathrm{g}}(\hat{k}_i,\hat{k}_{\mathrm{s}}) = \begin{cases}\displaystyle\sum_{n=-\infty}^{\infty}(-1)^n\zeta_n a_{n\mathrm{I}}\cos(n\varphi) & \text{for TE case,}\\ \displaystyle\sum_{n=-\infty}^{\infty}(-1)^n\zeta_n b_{n\mathrm{I}}\cos(n\varphi) & \text{for TM case,}\end{cases} \qquad (44)$$

where

$$\zeta_n = \begin{cases}2 \text{ for } n = 1,2,3\ldots,\\ 1 \text{ for } n = 0,\end{cases} \qquad (45)$$

and the expressions for $a_{n\mathrm{I}}$ and $b_{n\mathrm{I}}$ are given in Ref.[1].

In a similar way, the first-order scattered field of the Gaussian beam by cylinder #2 can be written as

$$\hat{p}\cdot\boldsymbol{E}^{\mathrm{s}}_{2\mathrm{c}}(\boldsymbol{r}) = H_0^{(1)}(k_0\rho_0)\exp(-\mathrm{i}\boldsymbol{k}_{\mathrm{s}}\cdot\boldsymbol{\rho}_2+\mathrm{i}\boldsymbol{k}_i\cdot\boldsymbol{\rho}_2)\hat{p}\cdot\bar{S}_2^{\mathrm{g}}(\hat{k}_i,\hat{k}_{\mathrm{s}}), \qquad (46)$$

where $\bar{S}_2^{\mathrm{g}}(\hat{k}_i, \hat{k}_{\mathrm{s}})$, which has a similar form as $\bar{S}_1^{\mathrm{g}}(\hat{k}_i, \hat{k}_{\mathrm{s}})$, is the bi-static scattered electric field amplitude vector of cylinder #2 when it is illuminated by the Gaussian beam.

Thus, the first-order scattered field from the cylinder-cylinder pair can be evaluated by Eqs.(43) and (46).

In the following part, we shall derive the solutions of the secondary scattered field.

Under the approximation that $\boldsymbol{E}_{\mathrm{ed}}$ and $\boldsymbol{H}_{\mathrm{md}}$ are considered as plane wave propagating along the $-\hat{k}_{\mathrm{s}}$ direction, in Eqs.(37) and (38) the expressions for $\boldsymbol{E}_{\mathrm{e2c}}$ and $\boldsymbol{H}_{\mathrm{m2c}}$ can be written as

$$\boldsymbol{E}_{\mathrm{e2c}}(\boldsymbol{r}) = \frac{-k_0 Z_0}{4} H_0^{(1)}(k_0\rho_0)\exp(-\mathrm{i}\boldsymbol{k}_{\mathrm{s}}\cdot\boldsymbol{\rho}_2) H_0^{(1)}(k_0\rho'')\bar{S}_{\mathrm{e2c}}^{p}(-\hat{k}_{\mathrm{s}}, \rho'')\,, \tag{47}$$

$$\boldsymbol{H}_{\mathrm{m2c}}(\boldsymbol{r}) = \frac{-k_0 Y_0}{4} H_0^{(1)}(k_0\rho_0)\exp(-\mathrm{i}\boldsymbol{k}_{\mathrm{s}}\cdot\boldsymbol{\rho}_2) H_0^{(1)}(k_0\rho'')\bar{S}_{\mathrm{m2c}}^{p}(-\hat{k}_{\mathrm{s}}, \rho'')\,, \tag{48}$$

where $\bar{S}_{\mathrm{e2c}}^{p}(-\hat{k}_{\mathrm{s}}, \rho'')$ and $\bar{S}_{\mathrm{m2c}}^{p}(-\hat{k}_{\mathrm{s}}, \rho'')$ are the electric and magnetic field bi-static scattering amplitude vector of cylinder #2 when it is illuminated by a plane wave.[26] ρ'' is the distance between the axis of cylinder #2 and the point at $\boldsymbol{\rho}$, that is $\rho'' = |\boldsymbol{\rho} - \boldsymbol{\rho}_2|$ and $\hat{\rho}'' = (\boldsymbol{\rho} - \boldsymbol{\rho}_2)/|\boldsymbol{\rho} - \boldsymbol{\rho}_2|$. Then, using Eqs.(37) and (38), we obtain the following two equations:

$$\hat{p}\cdot\boldsymbol{E}_{J12\mathrm{c}}^{\mathrm{s}} = \frac{-k_0 Z_0}{4} H_0^{(1)}(k_0\rho_0)\exp(-\mathrm{i}\boldsymbol{k}_{\mathrm{s}}\cdot\boldsymbol{\rho}_2)\int_{l_1} \boldsymbol{J}_1 \cdot H_0^{(1)}(k_0\rho'')\bar{S}_{\mathrm{e2c}}^{p}(-\hat{k}_{\mathrm{s}}, \rho'')\mathrm{d}l'', \tag{49}$$

$$\hat{q}\cdot\boldsymbol{H}_{\mathrm{m12c}}^{\mathrm{s}} = \frac{-k_0 Y_0}{4} H_0^{(1)}(k_0\rho_0)\exp(-\mathrm{i}\boldsymbol{k}_{\mathrm{s}}\cdot\boldsymbol{\rho}_2)\int_{l_1} \boldsymbol{M}_1 \cdot H_0^{(1)}(k_0\rho'')\bar{S}_{\mathrm{m2c}}^{p}(-\hat{k}_{\mathrm{s}}, \hat{\rho}'')\mathrm{d}l'', \tag{50}$$

where $\boldsymbol{J}_1$ and $\boldsymbol{M}_1$ denote the equivalent electric and magnetic current density on the surface of cylinder #1 respectively when illuminated by the incident Gaussian beam.

Keeping in mind the conditions on the dimensions of, and the distance between, the cylinders as specified in Eq.(35), we can evaluate analytically Eqs.(49) and (50). In Eqs.(49) and (50), noting that $\boldsymbol{\rho}$ is the position of the point on the surface of cylinder #1, then we have $|\boldsymbol{\rho}_2 - \boldsymbol{\rho}| \approx |\boldsymbol{\rho}_2 - \boldsymbol{\rho}_1|$, thus

$$\hat{\rho}'' = \frac{(\boldsymbol{\rho} - \boldsymbol{\rho}_2)}{|\boldsymbol{\rho} - \boldsymbol{\rho}_2|} \approx \frac{(\boldsymbol{\rho}_1 - \boldsymbol{\rho}_2)}{|\boldsymbol{\rho}_1 - \boldsymbol{\rho}_2|} = -\hat{\tilde{\rho}}\,. \tag{51}$$

Under this approximation, in Eqs.(49) and (50), $\bar{S}_{\mathrm{e2c}}(-\hat{k}_{\mathrm{s}}, \hat{\rho}'')$ and $\bar{S}_{\mathrm{m2c}}(-\hat{k}_{\mathrm{s}}, \hat{\rho}'')$ are not functions of the integration variables. Therefore, these two equations can be rewritten as

$$\begin{aligned}
\hat{p}\cdot\boldsymbol{E}_{J12\mathrm{c}}^{\mathrm{s}} &= \frac{-k_0 Z_0}{4} H_0^{(1)}(k_0\rho_0)\exp(-\mathrm{i}\boldsymbol{k}_{\mathrm{s}}\cdot\boldsymbol{\rho}_2)\bar{S}_{\mathrm{e2c}}^{p}(-\hat{k}_{\mathrm{s}}, -\hat{\tilde{\rho}})\cdot\int_{l_1}\boldsymbol{J}_1\cdot H_0^{(1)}(k_0\rho'')\mathrm{d}l'' \\
&= \frac{k_0 Z_0}{4} H_0^{(1)}(k_0\rho_0)\exp(-\mathrm{i}\boldsymbol{k}_{\mathrm{s}}\cdot\boldsymbol{\rho}_2)\bar{S}_{\mathrm{e2c}}^{p}(-\hat{k}_{\mathrm{s}}, -\hat{\tilde{\rho}})\cdot\Big[\hat{\tilde{\rho}}\times\hat{\tilde{\rho}}\times\int_{l_1}\boldsymbol{J}_1\cdot H_0^{(1)}(k_0\rho'')\mathrm{d}l''\Big], \qquad (52)\\
\hat{q}\cdot\boldsymbol{H}_{\mathrm{m12c}}^{\mathrm{s}} &= \frac{-k_0 Y_0}{4} H_0^{(1)}(k_0\rho_0)\exp(-\mathrm{i}\boldsymbol{k}_{\mathrm{s}}\cdot\boldsymbol{\rho}_2)\bar{S}_{\mathrm{m2c}}^{p}(-\hat{k}_{\mathrm{s}}, -\hat{\tilde{\rho}})\cdot\int_{l_1}\boldsymbol{M}_1\cdot H_0^{(1)}(k_0\rho'')\mathrm{d}l'' \\
&= \frac{-k_0 Y_0}{4} H_0^{(1)}(k_0\rho_0)\exp(-\mathrm{i}\boldsymbol{k}_{\mathrm{s}}\cdot\boldsymbol{\rho}_2)[-\hat{\tilde{\rho}}\times\bar{S}_{\mathrm{e2c}}^{p}(-\hat{k}_{\mathrm{s}}, -\hat{\tilde{\rho}})]\cdot\int_{l_1}\boldsymbol{M}_1\cdot H_0^{(1)}(k_0\rho'')\mathrm{d}l'' \\
&= \frac{-k_0 Y_0}{4} H_0^{(1)}(k_0\rho_0)\exp(-\mathrm{i}\boldsymbol{k}_{\mathrm{s}}\cdot\boldsymbol{\rho}_2)\bar{S}_{\mathrm{e2c}}^{p}(-\hat{k}_{\mathrm{s}}, -\hat{\tilde{\rho}})\cdot\Big[\hat{\tilde{\rho}}\times\int_{l_1}\boldsymbol{M}_1\cdot H_0^{(1)}(k_0\rho'')\mathrm{d}l''\Big]. \qquad (53)
\end{aligned}$$

Using Eqs.(52) and (53), we get the secondary scattered field $\hat{p}\cdot\boldsymbol{E}_{12\mathrm{c}}^{\mathrm{s}}$ from cylinder #2:

$$\begin{aligned}
\hat{p}\cdot\boldsymbol{E}_{12c}^{\mathrm{s}} &= \hat{p}\cdot(\boldsymbol{E}_{J12\mathrm{c}}^{\mathrm{s}} + \boldsymbol{E}_{\mathrm{m12c}}^{\mathrm{s}}) = H_0^{(1)}(k_0\rho_0)\exp(-\mathrm{i}\boldsymbol{k}_{\mathrm{s}}\cdot\boldsymbol{\rho}_2)\bar{S}_{\mathrm{e2c}}^{p}(-\hat{k}_{\mathrm{s}}, -\hat{\tilde{\rho}}) \\
&\quad\cdot\Big\{\frac{-k_0 Z_0}{4}\hat{\tilde{\rho}}\times\hat{\tilde{\rho}}\times\int_{l_1}\boldsymbol{J}_1\cdot H_0^{(1)}(k_0\rho'')\mathrm{d}l'' - \frac{k_0}{4}\hat{\tilde{\rho}}\times\int_{l_1}\boldsymbol{M}_1\cdot H_0^{(1)}(k_0\rho'')\mathrm{d}l''\Big\} \\
&\approx H_0^{(1)}(k_0\rho_0)\exp(-\mathrm{i}\boldsymbol{k}_{\mathrm{s}}\cdot\boldsymbol{\rho}_2 + \mathrm{i}\boldsymbol{k}_i\cdot\boldsymbol{\rho}_1)\bar{S}_{\mathrm{e2c}}^{p}(-\hat{k}_{\mathrm{s}} - \hat{\tilde{\rho}})\cdot H_0^{(1)}(k_0|\tilde{\rho}|)\bar{S}_{\mathrm{e1c}}^{\mathrm{g}}(\hat{k}_i, \hat{\tilde{\rho}})\,, \qquad (54)
\end{aligned}$$

where $\bar{S}_{\mathrm{e2c}}^{p}(-\hat{k}_{\mathrm{s}}, -\hat{\tilde{\rho}})$ is the bi-static scattered electric field amplitude vector of the cylinder #2 when it is illuminated by a plane wave and $\bar{S}_{\mathrm{e1c}}^{\mathrm{g}}(\hat{k}_i, \hat{\tilde{\rho}})$ is the scattered electric field amplitude vector of cylinder #1 when

the incident wave is a Gaussian beam. Meanwhile, in Eq.(54), the relation $\boldsymbol{E}^{\rm s}_{\rm m12s} = -Z_0\hat{k}_{\rm s} \times \boldsymbol{H}^{\rm s}_{\rm m12s}$ and the Stratton–Thu formulation are used.

Using the similar method, we can obtain the secondary scattered field from cylinder #1 as

$$\hat{p} \cdot \boldsymbol{E}^{\rm s}_{21c} \approx H_0^{(1)}(k_0\rho_0)\exp(-{\rm i}\boldsymbol{k}_{\rm s} \cdot \boldsymbol{\rho}_1 + {\rm i}\boldsymbol{k}_i \cdot \boldsymbol{\rho}_2)\bar{S}^p_{\rm e1c}(-\hat{k}_{\rm s}, \hat{\tilde{\rho}}) \cdot H_0^{(1)}(k_0|\tilde{\rho}|)\bar{S}^{\rm g}_{\rm e2c}(\hat{k}_i, -\hat{\tilde{\rho}})\,, \tag{55}$$

where $\bar{S}^p_{\rm e1c}(-\hat{k}_{\rm s}, \hat{\tilde{\rho}})$ is the bi-static scattered electric field amplitude of the cylinder #1 when it is illuminated by a plane wave, $\bar{S}^{\rm g}_{\rm e2c}(\hat{k}_i, -\hat{\tilde{\rho}})$ is the scattered electric field amplitude vector of cylinder #2 when the incident wave is a Gaussian beam. It should be noted that Eq.(55) can also be obtained from Eq.(54) by employing the relation given by Eq.(33). Thus, the total scattered field up to second-order is $(\hat{p} \cdot \boldsymbol{E}^{\rm s}_{1s} + \hat{p} \cdot \boldsymbol{E}^{\rm s}_{2s} + \hat{p} \cdot \boldsymbol{E}^{\rm s}_{12s} + \hat{p} \cdot \boldsymbol{E}^{\rm s}_{21s})$.

5. Numerical results

If the value of the beam-waist radius becomes big enough, the problem of a Gaussian beam is simplified to the problem of a plane wave. For the numerical electromagnetic code (NEC), which is a computational package based on the TDIFM, we have only provides results for plane wave. Therefore, to check the validity of the present method, the scattering results of a plane wave from two adjacent plasma-coated conducting cylinders are compared with the data obtained by using NEC.

Figure 3 gives the elevation patterns of bi-static scattering width for two homogeneous plasma-coated conducting cylinders when the polarization direction of the electric field is along the positive x-axis. The radii of cylinder #1 and #2 are both equal to 0.01m and the thickness of the plasma coating on the two cylinders is 0.005m. The position vectors of the cylinders are $\boldsymbol{\rho}_1 = (y_1, z_1) = (0\ {\rm m}, 0\ {\rm m})$ and $\boldsymbol{\rho}_2 = (y_2, z_2) = (0.05\ {\rm m}, 0.07\ {\rm m})$ respectively. Here the collision frequency and the electron density of the plasma are $V_{\rm e} = 50$ GHz and $N_{\rm e0} = 5.0 \times 10^{17}\ {\rm m}^{-3}$. The beam-waist radius is $w_0 = 100$ m and this value is big enough to reduce the problem of Gaussian beam to a problem of plane wave. From Fig.3, it is found that the phase difference between the scattered field from cylinder #1 and cylinder #2 is greater when the radar frequency is higher. Therefore, the curves of the scattered field oscillate intensively with the increase of radar frequency. Meanwhile, one can also see that the second-order result obtained by using our method provides a reasonable approximation and is in agreement with the TDIEM data over the angular range.

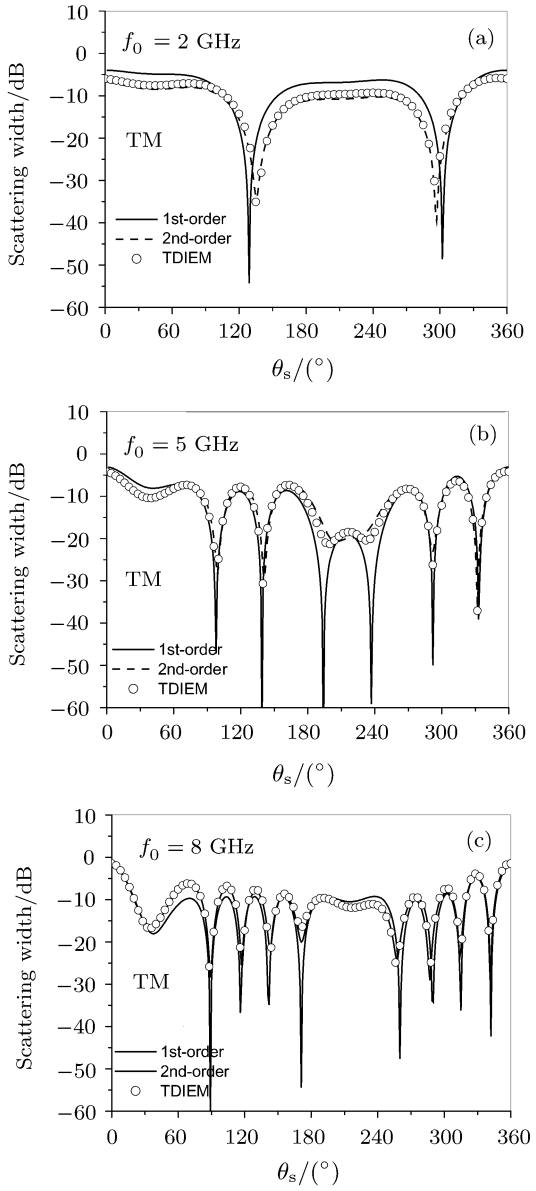


Fig.3. Bi-static scattering width of two parallel adjacent cylinders versus scattering angle $\theta_{\rm s}$ for different radar frequencies.

Figure 4 gives the elevation patterns of bi-static scattering width for two homogeneous plasma-coated conducting cylinders when the polarization direction

of the electric field is along the positive y-axis. Here, the other parameters are the same as those in Fig.3. As shown in Fig.4, it is obvious that the effect of the secondary scattered field becomes smaller with the increase of the separation between the two cylinders. In Fig.4, it is shown that when the separation between the two cylinders is 0.2 m, in this case, the two cylinders are located far enough apart, the secondary scattering field shows very little effect on the composite field and the first- and second-order scattering results are both in agreement with the TDIEM computation results. From Fig.4, it is also obvious that the second-order result provides a reasonable approximation for different separations.

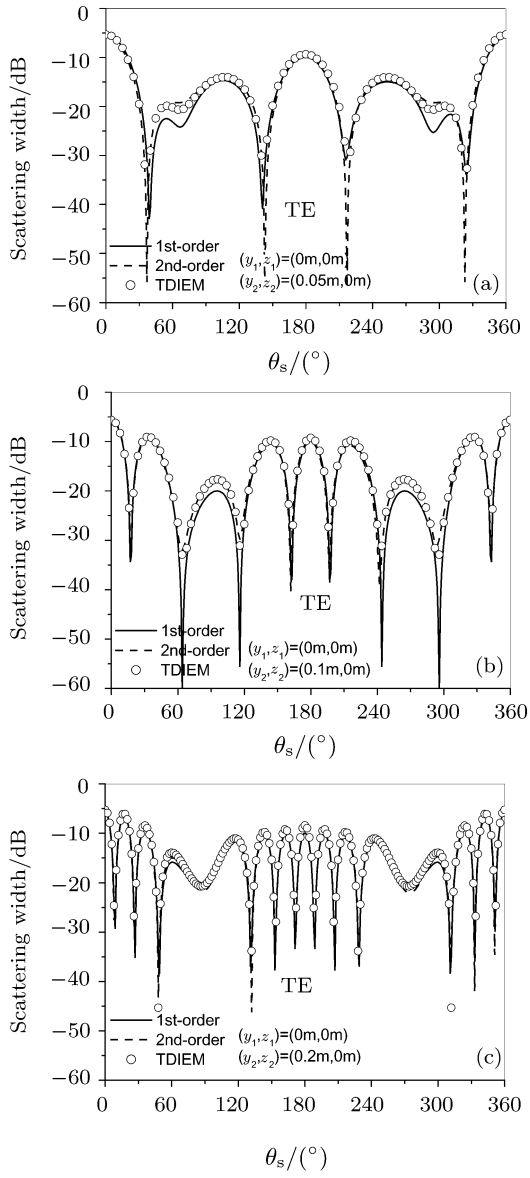


Fig.4. Bi-static scattering width of two homogeneous plasma-coated conducting cylinders for various separations.

In the following discussion, the problem of scattering of Gaussian beam by two inhomogeneous plasma-coated conducting cylinders is considered. To deal with this type of problem, the inhomogeneous plasma coating can be divided into many uniform plasma layers. Suppose that the electron density profile of the inhomogeneous plasma coating takes the form of parabola distribution along radial direction. The electron density of each layer can be expressed as $N_e(i) = N_{e_0} - N_{e_0}[r_i - r_0/d]^2$, where N_{e_0} is the centre electron density and $N_e(i)$ denotes electron density of the ith layer, r_0 and r_i are the radii of the conducting cylinder and the ith layer respectively, and d denotes the thickness of the inhomogeneous plasma coating.

In Fig.5, the radii of the conducting cylinder #1 and #2 are both 0.5m, the incident radar frequency is 5GHz and the polarization direction of the electric field is along the positive y-axis (TE). The position vectors of the cylinders are $\boldsymbol{\rho}_1 = (y_1, z_1) = (0\text{m}, 0\text{m})$ and $\boldsymbol{\rho}_2 = (y_2, z_2) = (3.0\text{m}, 4.0\text{m})$ respectively. The beam-waist radius is $w_0 = 0.5$ m. Here, the other parameters are the same as those in Fig.3. From Fig.5, one can observe that the attenuation of the scattering width between the angular ranges from 20° to 340° is very obvious. And it is also shown that the attenuation of the scattering width becomes stronger with the increasing thickness of the plasma coating.

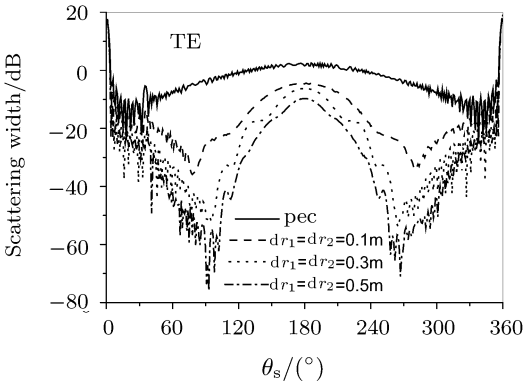


Fig.5. Angular distribution of the bi-static scattering width for different thicknesses of the plasma coating.

Figure 6 gives the backscattering width versus the radar frequency for different centre electron densities. The radius of the cylinders and the thickness of the inhomogeneous plasma coatings are 0.3 m and 0.05 m, respectively. The position vectors of the cylinders are $\boldsymbol{\rho}_1 = (y_1, z_1) = (0\text{m}, 0\text{m})$ and $\boldsymbol{\rho}_2 = (y_2, z_2) = (1.4\text{m}, 1.7\text{m})$ respectively. The other parameters are the same as those in Fig.5. As shown in Fig.6, with

the increase of the centre electron density, the attenuation of the backscattering width is greater and the attenuation bandwidth is broadened. This phenomenon can be explained by the reason that higher electron density will cause more intense collision between electron and the other particles and then the absorption of the plasma layer becomes stronger. Because the cutoff frequency of the plasma layer increases for the increasing centre electron density, from Fig.6, it is also observed that the radar frequency, which corresponds to the minimum value of the backscattering width, is increscent with the increase of the electron density of the plasma coating.

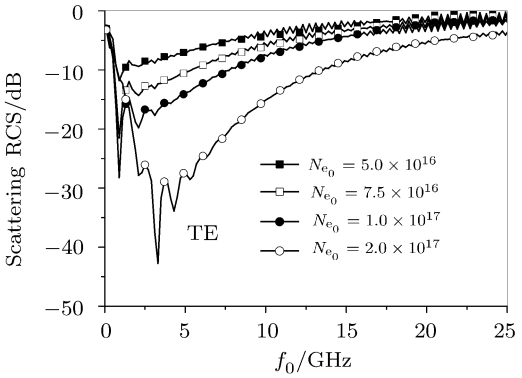


Fig.6. Backscattering width versus radar frequency f_0 for various centre electron densities.

In Fig.7, the radius of the cylinders is 0.1 m, the position vectors of the cylinders are

$$\boldsymbol{\rho}_1 = (y_1, z_1) = (0\text{m}, 0\text{m})$$

and

$$\boldsymbol{\rho}_2 = (y_2, z_2) = (0.4\text{m}, 0.7\text{m})$$

respectively. And the other parameters are the same as those in Fig.3. From Fig.7, one can observe that with the increase of the thickness of the plasma layer, the attenuation of the backscattering width is stronger. However, for different thicknesses of the plasma layer, the collision frequency, which corresponds to the minimum value of the backscattering width, is a constant value, which is equal to the angular frequency of the incident beam. This is because that when collision frequency of the plasma is equal to the angular frequency of the incident wave, resonance absorption will occur. Figure 8 gives the backscattering width versus collision frequency for various electron densities. Here, the other parameters are the same as those in Fig.7. From Fig.8, it is obvious that the attenuation of the backscattering width is stronger if the electron density is higher. From Figs.7 and 8, for a given radar beam, it can also be seen that the resonance attenuation only depends on the collision frequency of the plasma.

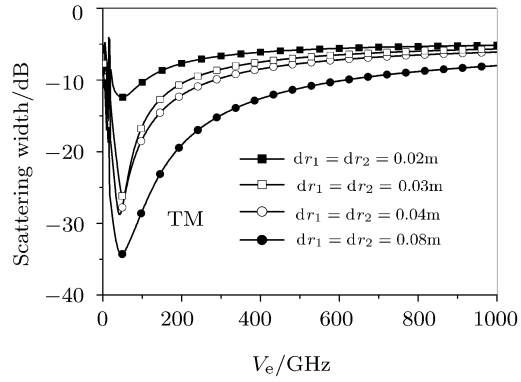


Fig.7. Backscattering width versus collision frequency V_e for different thickness of the coated plasma layer.

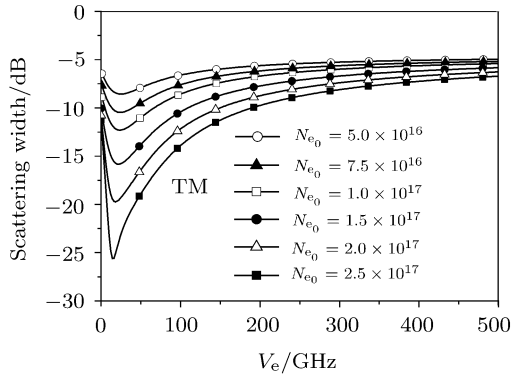


Fig.8. Backscattering width versus collision frequency V_e for different electron density.

6. Conclusions

In this paper, based on the equivalence principle and the reciprocity theorem, a general technique has been developed for deriving the scattered field up to second order from two parallel 2D targets. And the relation of the secondary scattered field from target #1 and target #2 is obtained. Specifically, the formulations are applied to obtain approximate analytical solutions for the second-order scattered fields of Gaussian beam from two adjacent plasma-coated circular cylinders. The validity of the present method

was verified by comparison with the time domain integral equation computations, and agreement is obtained. Meanwhile, the effects of the electron density, collision frequency and thickness of the plasma layer on the scattering width are discussed in detail and some significant conclusions are obtained. It should be pointed out that the method proposed in this paper can also be extended to the problem of the electromagnetic scattering from 3D targets.

References

[1] Wu Z S and Guo L X 1998 *Progress In Electromagnetics Research PIER* **18** 317

[2] Zimmermann E, Dandliker R and Souli N 1995 *J. Opt. Soc. Am.* A **12** 398

[3] Chen H C and Cheng D K 1964 *IEEE Trans. Antennas Propagat.* **12** 348

[4] Wu X and Wei R 1995 *Radio Sci.* **30** 403

[5] Wu Z S and Guo L X 1997 *Appl. Opt.* **36** 5188

[6] Gouesbet G, Grehan G and Maheu B 1990 *J. Opt. Soc. Am.* A **7** 998

[7] Doicu A and Wriedt T 1997 *Appl. Opt.* **13** 2971

[8] Wang N 1985 *IEEE Trans. Antennas Propagat.* **33** 960

[9] Han Y P and Wu Z S 2000 *Acta Phys. Sin.* **49** 57 (in Chinese)

[10] Bai L, Wu Z S, Chen H and Guo L X 2005 *Acta Phys. Sin.* **54** 2025 (in Chinese)

[11] Wu P, Han Y P and Liu D F 2005 *Acta Phys. Sin.* **54** 2676 (in Chinese)

[12] Han Y P 2005 *Acta Phys. Sin.* **54** 5139 (in Chinese)

[13] Yokota M, Takenaka T and Fukumitsu O 1986 *J. Opt. Soc. Am.* A **3** 580

[14] Elsherbeni A Z and l Hamid M 1987 *IEEE Trans. Antennas Propaga.* **35** 355

[15] Hongo K 1978 *IEEE Trans. Antennas Propagat.* **26** 748

[16] Sarabandi K and Polatin P F 1994 *IEEE Trans. Antennas Propagat.* **42** 510

[17] Li S Q, Fang J and Wang W B 1998 *IEEE Trans. Geosci. Remote Sensing* **26** 1981

[18] Chiu T C 1998 *Electromagnetic Scattering from Rough Surface Covered with Short Branching Vegetation* (Ph.D. Dissertation, the University of Michigan, Ann Arbor) p46

[19] Kong J A 2000 *Electromagnetic Wave Theory* (New York: Wiley) p649

[20] Laroussi M 1993 *IEEE Trans. Plasma Sci.* **24** 366

[21] Liu S B, Mo J J and Yuan N C 2002 *Int. J. Inf. MM Waves* **23** 1803

[22] Tang D L and Sun A P 2003 *IEEE Trans. Plasma Sci.* **31** 405

[23] Vidmar R J 1990 *IEEE Trans. Plasma Sci.* **18** 733

[24] Chang Y and Harrington R F 1977 *IEEE Trans. Antennas Propagat.* **25** 789

[25] Wang M G 1994 *Geometrical Theory of Diffraction* (Xi'Dian University Xi'an) p81 (in Chinese)

[26] Ruck G T 1970 *Radar Cross Section Handbook* (New York: Plenum) p205